A Chloroquine-resistant Swiss 3T3 Cell Line with a Defect in Late Endocytic Acidification

Cynthia Corley Cain and Robert F. Murphy

Department of Biological Sciences and Center for Fluorescence Research in Biomedical Sciences, Carnegie-Mellon University, Pittsburgh, Pennsylvania 15213

Abstract. To investigate the role of acidification in cell proliferation, several cell lines resistant to chloroquine were isolated with the expectation that some would express altered endocytic acidification. The preliminary characterization of one of these lines, CHL60-64, is described. In contrast to endocytic mutants described previously, the initial phase of endocytic acidification, as measured by transferrin acidification, is normal in this cell line. However, a difference in subsequent endocytic acidification was observed in CHL60-64. In the parental cells, internalized dextran was fully acidified to approximately pH 5.5 within 1 h. In CHL60-64, the pH in the endocytic compartment was only 6.1 after 1 h and remained as high as 5.8 for at least 4 h. After an 8-h incubation, the pH decreased to 5.5, indicating that the second phase of acidification is only slowed in CHL60-64, and not blocked. Consistent with this retarded acidification, ATP-dependent acidification in vitro (as measured by acridine orange accumulation) was reduced in both the lysosomal fraction and the endosomal fraction isolated from CHL60-64. A decrease in the in vivo rate of acridine orange accumulation after perturbation with amine was also observed. In addition to amine resistance and defective acidification, CHL60-64 was found to be resistant to vacuolation in the presence of chloroquine and ammonium chloride, and was resistant to ouabain. Further studies on this new class of endocytosis mutant, in combination with existing mutants, should help to clarify the mechanisms responsible for the regulation of endocytic acidification.

MANY viruses and toxins require internalization and exposure to an acidic pH in order to penetrate into the cytosol (8, 20, 24). A number of cell lines that are defective in endocytosis and/or endocytic acidification have been isolated by taking advantage of this fact. Robbins et al. (6, 15, 16, 19) have described a number of cell lines, selected for diphtheria toxin resistance and impaired mannose-6-phosphate receptor activity, that are resistant to infection by Sindbis virus and vesicular stomatitis virus, as well as protein toxins. Some mutants were found to be defective in the uptake of iron from transferrin, a phenotype linked to their defect in vacuolar acidification, and some exhibited altered Golgi apparatus functions as well. Selection for resistance to both modeccin and diphtheria toxin enabled Draper and co-workers (7, 22) to isolate Chinese hamster ovary cell lines that were temperature sensitive for viability, resistance to protein toxins (diphtheria toxin, modeccin, *Pseudomonas* exotoxin A), and ATP-stimulated acidification of endocytic vesicles. The temperature-sensitive lesion in viability could be overcome by the addition of $FeSO_4$ to the growth media. Merion et al. (9) have characterized Chinese hamster ovary acidification mutants resistant to *Pseudomonas* exotoxin A, which were found to be cross-resistant to diphtheria toxin and several animal viruses. Monensin-resistant mutants have been isolated that are cross-resistant to vesicular stomatitis virus (13); however, this resistance appears to be unrelated to acidification. With the exception of one of the mutants characterized by Merion et al. (9), which showed decreased acidification of both compartments, all of the acidification mutants described to date were found to have defects in early (endosomal) but not late (lysosomal) acidification.

There is considerable biochemical evidence, in support of this genetic evidence, indicating that the mechanisms of endosomal and lysosomal acidification have distinct features. Although both endosomes and lysosomes maintain an acidic pH through an ATP-dependent process, the extent of acidification in endosomes is less than that in lysosomes both in vivo (11, 17, 18) and in vitro (15, 22). In vivo acidification of endocytosed ligands by 3T3 cells is biphasic, with a rapid early acidification to pH 6.1, and a subsequent late acidification to below pH 5.5. The two phases are differentially sensitive to reduced temperature, as only the second phase of acidification is inhibited between 13° and 17°C (17).

A common factor in the mutant selection schemes described previously is the use of selective agents which must be endocytosed. This may favor selection of mutants in the early stages of endocytosis and acidification. We have previously shown that weak bases, such as chloroquine and ammonium chloride, exert both a growth inhibitory and toxic effect on cell cultures; these effects show a strong correlation

with an increase in pH in endocytic vesicles (2). In order to obtain new types of acidification mutants, chloroquine resistance was used as a selection. The initial characterization of chloroquine-resistant mutant CHL60-64 is described in this paper. Unlike acidification mutants previously described, this cell line is not defective in the initial phase of endocytic acidification, but shows a defect in subsequent endocytic acidification, providing further evidence that the acidification mechanisms in these two phases are distinct.

Materials and Methods

Mutant Isolation

All reagents were obtained from Sigma Chemical Co. (St. Louis, MO) unless otherwise indicated.

To enrich for chloroquine-resistant mutants, Swiss albino 3T3 fibroblasts were grown continuously in Dulbecco's modified Eagle's medium (Gibco, Grand Island, NY) supplemented with 10% fetal bovine serum (Gibco), 100 U/ml penicillin, 100 μg/ml streptomycin, and 2 mM L-glutamine (cDMEM)[1] supplemented with 30 μM chloroquine. All cultures were refed at 2–3-d intervals. To select for resistant cells, subcultures were plated at 1.5×10^5 cells per 75 cm^2 flask, and refed 1 d later with cDMEM containing 60 μM chloroquine. Resistant colonies were harvested (after 2 wk) by trypsinization, and cultured continuously in cDMEM with 60 μM chloroquine. Clones were obtained by limiting dilution. All subsequent experiments were done using cultures of one of these clones, CHL60–64, which had been grown in the presence of 60 μM chloroquine for 4 mo, then passaged without chloroquine for 2–4 wk. To control for possible effects of the high passage number of this cell line (~160), a parental cell line with the same passage number was used in the characterization experiments.

Growth Curves

Amine resistance was determined essentially as described previously (2). Cells were plated at a density of 1×10^4 per 60 mm plate in 5 ml cDMEM. The cultures were refed with cDMEM supplemented with various concentrations of amine 1 and 3 d later. Initial counts were made 1 d after plating to determine the plating efficiency (~65%) and the samples incubated with amine were counted 4 d after plating. The number of cell divisions was calculated relative to the number of cells at the time of amine addition.

To determine ouabain resistance, cells were plated as described above. Fresh media containing appropriate concentrations of ouabain was added 1 and 4 d after plating, and cell counts were made 1 d later.

Dextran Acidification

Late endocytic acidification was measured using the fluorescein-rhodamine method described previously (2, 11). Dextran conjugated with both FITC and substituted rhodamine isothiocyanate (XRITC) (FITC/XRITC-dextran) was prepared by the dibutyltin-dilaurate method (3) with a molar ratio of 2:1 XRITC/FITC. Cells were plated at a density of 1×10^5 on 60 mm plates in 5 ml cDMEM 2 d before use. The cultures were incubated with either a mixture of 1 mg/ml FITC-dextran and 2 mg/ml XRITC-dextran, or with 4 mg/ml FITC/XRITC-dextran in 1.5 ml incubation media, washed eight times with PBS containing 0.9 mM Ca^{2+} and 0.5 mM Mg^{2+} (PBS/Ca/Mg), and incubated for various times in the absence of dextran. Cells were harvested by scraping and analyzed at room temperature by flow cytometry. Data for 20,000 live cells (selected on the basis of a forward scatter threshold) were collected for each sample. The signal to autofluorescence ratio was at least 10:1 for the rhodamine fluorescence and 5:1 for the fluorescein fluorescence.

Transferrin Acidification

The acidification kinetics of transferrin were used as a measure of early endocytic acidification. The method used has been described in detail elsewhere (21). Briefly, cells were labeled at 4°C for 30–40 min with 10 μg/ml FITC-transferrin and lissamine rhodamine sulfonyl chloride-conjugated transferrin (LRSC-transferrin). Excess transferrin was removed by washing the sample with PBS/Ca/Mg, the cells were harvested by scraping, and initial fluorescence was determined by flow cytometry. The samples were then rapidly warmed to 37°C, and analysis continued. Average values for all parameters were calculated over 30-s intervals (~4,500 cells per interval). The percent of transferrin remaining external was determined using polyclonal FITC-conjugated goat anti-human transferrin antibody (a kind gift of Tago, Inc., Burlingame, CA) in a parallel experiment.

In Vitro Acridine Orange Uptake

To measure the acidification phenotype of CHL60-64 in vitro without requiring endocytosis of a probe, the accumulation of the metachromatic dye acridine orange (AO; Kodak Laboratory and Specialty Chemicals, Eastman Kodak Co., Rochester, NY) was measured in isolated vesicles. Cells were plated on 150 mm dishes and grown to confluence with refeeding every 3 d. After 7 d, the cells were harvested by scraping, washed, and homogenized at 4°C with a Potter-Elvehjm homogenizer, then spun at 1,000 *g* for 10 min to remove unbroken cells and nuclei. Postnuclear supernatants from $4–8 \times 10^7$ cells in 7 ml homogenization buffer (HB; 0.25 M sucrose, 2 mM EDTA, 10 mM Hepes, adjusted to pH 7.3 with NaOH) were mixed with a Percoll stock solution in HB for a final concentration of 27% (vol/vol) Percoll 14 ml gradient. The gradients were centrifuged at 25,000 *g* (maximum) for 151 min with a SA600 rotor in a RC5C centrifuge (Sorvall Instruments Div., E. I. Du Pont de Nemours & Co., Inc., Newtown, CT), 0.4 ml fraction were collected; lysosomal fractions (fractions 1–6; average density 1.09) and endosomal fractions (fractions 24–29; average density 1.05) were determined as the heavy and light peaks of acid phosphatase activity. Protein concentrations of the pooled fractions were measured as the absorbance at 280 nm corrected for the scatter due to the Percoll in the fractions.

AO uptake was determined using the method of Marnell et al. (7). Vesicle fractions (800 μg protein) were diluted to 2 ml in histidine buffer (30 mM histidine, 130 mM NaCl, 20 mM KCL, 2 mM $MgCl_2$, pH 7.0) and incubated at room temperature for 1 h. 5 μl of 1 mM AO in histidine buffer were added (final concentration of 2.5 μM), and the sample further incubated for 5 min to allow equilibration. AO uptake into vesicles was measured as the change in the difference between the absorbance at 492 and 540 nm ($\Delta A_{492-540}$) at 15-s intervals using a Gilford Response spectrophotometer (Ciba-Corning Diagnostics Corp., Oberlin, OH) or an 8452A diode array spectrophotometer (Hewlett-Packard Co., Palo Alto, CA). After initial values for the two absorbances were determined, 5 μl of 800 mM Mg-ATP were added (final concentration, 2 mM), and analysis continued for 30 min. After analysis, 5 μl of 4 mM monensin were added to dissipate any pH gradients.

In Vivo Acridine Orange Uptake

The procedures used will be described in detail elsewhere (Yaacobi, M., C. C. Cain, D. McCaslin, and R. F. Murphy, manuscript in preparation). 2×10^5 cells were plated on 25 cm^2 flasks 2 d before use. Cells were suspended by trypsinization, diluted to 1×10^6 cells/ml in PBS/Ca/Mg, and 20 μl/ml unlabeled 7.5 μm polystyrene beads (Flow Cytometry Standards Corporation, Research Triangle Park, NC) were added. After a baseline (autofluorescence) was determined for the sample, AO was added to a concentration of 200 ng/ml (0.663 μM), and AO uptake monitored for 15 min. Ammonium chloride was added from a 10-fold concentrated stock in PBS/Ca/Mg and the sample further analyzed for 15 min. Logarithmic amplifiers were used for all fluorescence parameters in order to accurately record the large changes in fluorescence observed (data were converted to linear scale before further analysis). Sample temperatures were maintained at 37°C, while ~150 events/s were collected. A threshold on side scatter was used to record data for both cells and beads. Upper and lower forward scatter gates were used in the analysis of the data in order to separately analyze the fluorescence from live cells and beads. Background fluorescence from the AO in solution was determined by analysis of the apparent fluorescence of the unlabeled beads, and was ~2% of the green signal. No red signal due to AO fluorescence was seen for the beads at this concentration. The signal to autofluorescence ratio was ~7:1 for the red fluorescence, and >1,000:1 for the green fluorescence.

Flow Cytometry

A modified FACS 440 with a Consort 40 computer system (Becton Dickinson FACS Systems, Mountain View, CA) was used for all flow cytometric analyses. Excitation was with the 488-nm line (40 mW) from an argon ion

1. *Abbreviations used in this paper*: AO, acridine orange; cDMEM, complete Dulbecco's modified Eagles medium; LRSC, lissamine rhodamine sulfonyl chloride; XRITC, substituted rhodamine isothiocyanate.

laser and the 568-nm line (60 mW) from a krypton ion laser. Green fluorescence was measured using a 530-nm band-pass filter (30 nm bandwidth) and a photomultiplier tube (model 9924A; EMI, Inc., Clinton, CT) with a high voltage of either 700 (FITC/XRITC-dextran) or 400 V (AO). Red fluorescence was measured using a 625-nm band-pass filter (35 nm bandwidth) and a photomultiplier tube (model 4001-06-300; Hamamatsu Corp., Middlesex, NJ) with a high voltage of either 700 (FITC/XRITC-dextran) or 800 V (AO).

Microscopy

Cells were plated at a density of 2×10^4 cells per well on two-chamber tissue culture chamber slides (Lab-Tek; Miles Scientific Div., Miles Laboratories, Inc., Naperville, IL) in 2 ml cDMEM 1 d before use. NH_4Cl or chloroquine was added from 10-fold concentrated stocks, and the cells incubated at 37°C for the indicated times. Phase contrast micrographs were taken using a 40× water immersion objective.

Results

Isolation of Chloroquine-resistant Cell Lines

To enrich for potential chloroquine-resistant cells, Swiss albino 3T3 cell cultures were grown continuously in the presence of 30 μM chloroquine. This concentration inhibited cell growth ~40% in continuously growing cultures (Fig. 1). After 3 mo of enrichment, subcultures were refed with 60 μM chloroquine, a concentration that caused death in the parental cell line. The frequency of resistant cells in the enriched population was $\sim 10^{-6}$. Stable cell lines resistant to higher concentrations of chloroquine (100–300 μM) have not yet been obtained. One of the clones resistant to 60 μM chloroquine, CHL60-64, was chosen for further characterization.

As shown in Fig. 1 *A*, the cell line CHL60-64 is significantly more resistant to chloroquine than the parental cells. This cell line grew well in 60 μM chloroquine, while there was cell death in the parental samples after only 3 d. CHL60-64 was also able to grow in 100 μM chloroquine. The chloroquine resistance is a stable phenotype, as CHL60-64 exhibited comparable resistance when cultured without selective pressure for up to 2 mo (data not shown). CHL60-64 also exhibits enhanced resistance to ammonium chloride (Fig. 1 *B*), suggesting that the mechanism of chloroquine resistance is not specific for chloroquine.

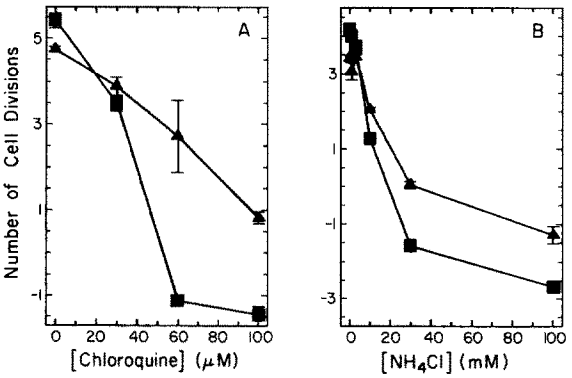

Figure 1. Chloroquine and ammonia resistance of CHL60-64. Actively growing cultures of high passage Swiss 3T3 (■) or CHL60-64 (▲) were incubated in the presence of chloroquine (*A*) or ammonium chloride (*B*) for 3 d, and the number of cell divisions calculated relative to the number of cells at the time of amine addition. Each point represents the average and standard deviation of two counts each on duplicate plates.

Acidification of Endocytosed Probes

Since the uptake of chloroquine requires acidic intracellular organelles, one of the anticipated phenotypes of resistant cell lines was defective intravesicular acidification. CHL60-64 exhibited a number of alterations related to acidification. The first was in the kinetics of the acidification of the fluid phase endocytic marker, dextran (Fig. 2 *A*). After a 30-min pulse and a 30-min chase, endocytosed dextrans were acidified to pH 5.6 by the parental cells. The pH remained essentially unchanged for up to 8 h. In the CHL60-64 samples however, the pH was only 6.1 after 1 h, and remained as high as 5.8 after 4 h. Eventually (after 8 h) the pH reached the same level as that of the parental cells.

To determine if this represented a general defect in acidification or a defect specific to late (lysosomal) acidification, early endocytic acidification kinetics were measured using fluorescent derivatives of transferrin according to procedures described previously (21). Cells were surface labeled with FITC- and LRSC-transferrin at 4°C, then warmed to 37°C to initiate synchronized endocytosis of the probes. The fluorescence values were corrected for the fluorescence due to transferrin remaining on the cell surface, and the ratio of

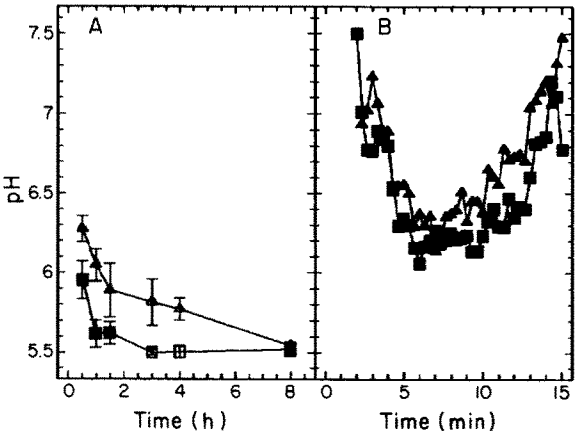

Figure 2. Endocytic acidification measurements. (*A*) Average lysosomal pH was calculated from measured FITC/XRITC fluorescence ratios for high passage Swiss 3T3 (■, □) or CHL60-64 (▲, △). Cells were incubated for 30 min (*solid symbols*) or 2 h (*open symbols*) in cDMEM supplemented with labeled dextrans, then washed, and the dextrans chased into lysosomal compartments by further incubation for various periods of time. Points represent the average and standard error of the mean of two to six samples. No difference in the total uptake of dextrans by these two cell lines was observed. (*B*) Transferrin acidification kinetics were determined for samples of Swiss 3T3 (■) or CHL60-64 (▲). The cells were cooled to 4°C and incubated with a mixture of FITC and LRSC transferrin at 4°C, washed, scraped, and analyzed. After establishing a baseline value for green and red fluorescence at the external pH, the cells were warmed to 37°C. To determine the pH of the internalized transferrin, the total fluorescence was corrected for the percent of the transferrin remaining on the cell surface, and the ratio of green fluorescence to red fluorescence was converted to pH using a standard curve. Points represent average values calculated for 30-s intervals. The data presented are representative of eight separate experiments for each cell type.

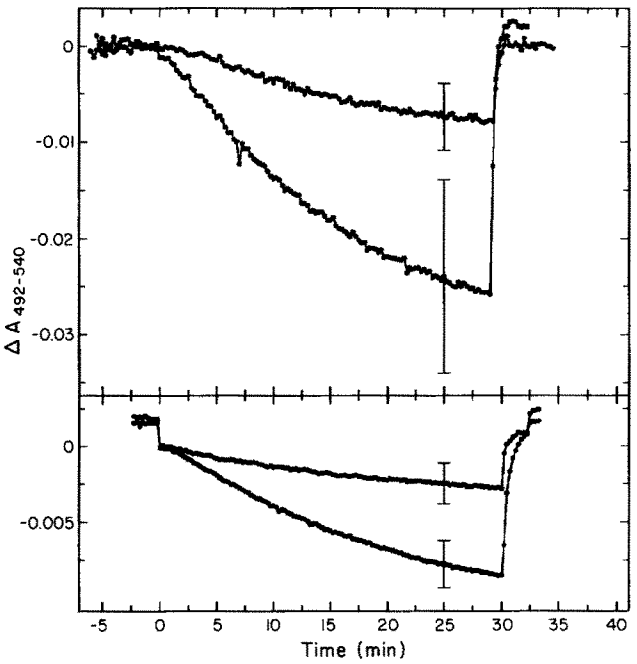

Figure 3. Acidification in isolated vesicles in vitro. The quenching of AO absorbance at 492 nm due to accumulation of the dye in acidic vesicles was measured for isolated lysosomes (*top* panel) and endosomes (*bottom* panel) in CHL60-64 (*upper curves*) and parental samples (*lower curves*). After incubation at room temperature for 1 h to dissipate existing proton gradients, samples were equilibrated with 2.5 μM AO and initial absorbance values were determined. ATP was added to a concentration of 2 mM in order to initiate acidification. Monensin was added to a concentration of 10 μM in order to collapse the pH gradients after 30 min. The lines show average values for two (endosomal) or three (lysosomal) separate experiments (standard deviations are shown at 25 min). The change in absorbance ($\Delta A_{492-540}$) was calculated relative to the absorbance recorded immediately after AO addition.

green fluorescence (FITC-transferrin) to red fluorescence (LRSC-transferrin) was converted to pH using a standard curve. Upon warming, the internalized transferrin was rapidly exposed to a pH of ~6.1 within 5 min (Fig. 2 *B*). The pH then rapidly increased to neutrality as the transferrin was recycled. No difference was seen in the transferrin acidification and alkalinization kinetics for the two cell lines, or in the kinetics of internalization of the ligand (data not shown). In contrast, the endosomal acidification mutant G.7.1 (7, 22) showed negligible acidification of transferrin at the nonpermissive temperature using the same procedure, while its parental cell line showed normal acidification (data not shown).

Acidification in Isolated Vesicles In Vitro

Since transferrin acidification in CHL60-64 is normal, the acidification defect would appear to be specific for late acidification. However, the decreased rate of late acidification observed in CHL60-64 could also be due to a decreased rate of transport of endocytosed material from mildly acidic endosomal compartments to more acidic lysosomal compartments. To distinguish between these two possibilities, and to more rigorously determine the acidification mechanism affected in CHL60-64, AO accumulation was measured in vitro in isolated endosomal and lysosomal fractions. This method does not require endocytosis of a probe for delivery to acidic intracellular compartments. AO is a weak base which accumulates in acidic vesicles via the same mechanism as vacuologenic amines such as chloroquine and ammonia. The protonated form of the base is much less membrane permeant than the unprotonated form. As a result, the protonated form of the base is trapped in any compartments that are acidic relative to the incubation media. The concentration of AO within a vesicle is dependent on the magnitude of the pH gradient across the vesicular membrane. At high concentrations, AO forms dimers and higher order multimers resulting in a spectral shift in absorbance and fluorescence from green to red. The difference between the absorbance at 492 and 540 nm is a measure of the accumulation of AO in the vesicles within the fractions. We have found in vitro that a concentration >15 μg/ml is required for the formation of the red fluorescent form of AO.

Postnuclear supernatants from 7-d confluent cells were prepared, and endosomal and lysosomal fractions were separated by density gradient centrifugation. The two fractions were identified as heavy and light peaks of acid phosphatase activity. No difference was seen in the relative distributions or extent of accumulation of either acid phosphatase or β-hexosaminidase in the two cell lines (data not shown). A reduction in the extent of acidification was seen for both the lysosomal and endosomal fractions from CHL60-64 (Fig. 3). The rate and extent of acidification after ATP addition were estimated by least squares exponential fitting. The average values for the maximum change in absorbance ($\Delta A_{492-540}$), rate constants ($t_{1/2}^{-1}$ min^{-1}), and initial rates are shown in Table I. In both vesicle fractions, the rate constants were similar for the parental cell line and CHL60-64. However, the maximum change in absorbance was 2.8-fold higher in the parental lysosomal fraction than it was in the mutant lysosomes, and 2.6-fold higher in the parental endosomal fractions than in those from the mutant.

Amine-induced Vacuolation

In addition to increasing the intravesicular pH, both chloro-

Table I. In Vitro Acidification of Vesicles Isolated from CHL60-64 and Parental Cells

	Lysosomes			Endosomes		
Cell Line	$\Delta A_{492-540}$	k (min^{-1})*	Initial rate	$\Delta A_{492-540}$	k (min^{-1})*	Initial rate
	$\times 10^2$	$\times 10^2$	$\times 10^4$	$\times 10^2$	$\times 10^2$	$\times 10^4$
Parental	3.6 ± 1.5	5.3 ± 2.2	18 ± 9.7	1.3 ± 0.3	4.3 ± 0.7	5.2 ± 0.4
CHL60-64	1.3 ± 0.9	5.0 ± 1.9	5.3 ± 1.9	0.5 ± 0.03	4.8 ± 0.1	2.3 ± 0.1

* First order rate constant.

quine and ammonium chloride induce the formation of large cytoplasmic vacuoles. This is a result of the accumulation of large concentrations of the protonated form of the amines due to the active acidification of vesicles in response to an increase in intravesicular pH (14). Since AO accumulates within acidic vesicles in a manner identical to the vacuologenic amines, low concentrations (200 ng/ml) of AO were added with the amines in order to estimate the kinetics of amine accumulation in vivo. This was measured in whole cells using flow cytometry.

To measure the in vivo AO accumulation for the parental and CHL60-64 cell lines, monolayers were suspended in PBS/Ca/Mg by scraping, and AO was added to a concentration of 200 ng/ml. Accumulation was monitored on a cell by cell basis as the increase in red and green fluorescence with time. The green fluorescence (excitation 488, emission 530) is a measure of the total cell-associated AO (a function of both the pH of the vesicles and the total volume), while the red fluorescence (excitation 568, emission 625) is a measure of the extent to which the AO has been concentrated within the cell. Although the concentration of AO within the cells cannot be calculated directly, the appearance of red fluorescence indicates that some organelles within the cell concentrate AO at least 75-fold (from 200 ng/ml to 15 μg/ml). (This corresponds to a pH of 5.5 relative to an external pH of 7.4.) In the absence of perturbation by amine, the rate and extent of AO uptake were quite similar in the two cell lines. This result is consistent with the dextran acidification data, as the initial uptake of AO is dominated by the steady state pH of all acidic vesicles (this result eliminates the possibility that the amine and drug resistance of CHL60-64 is the result of a change in membrane permeability).

When a high concentration of a vacuologenic amine (e.g., 100 mM ammonium chloride) was added, the red fluorescence dropped immediately to background levels and remained there for at least 15 min. This was observed for both cell types. The green fluorescence also dropped in both cell types but only transiently. In the parental cell cultures, the green fluorescence began almost immediately to increase exponentially, recovering within 15 min to a value 79% higher on average than the initial value (Fig. 4). This recovery above the initial value was also seen when 100 mM methylamine was used to perturb the pH gradients in the parental cells (Yaacobi, M., C. C. Cain, D. McCaslin, and R. F. Murphy, manuscript in preparation). The initial levels of AO fluorescence were similar in the wild-type and CHL60-64 cells, and the fluorescence decreased to the same extent upon addition of ammonium chloride. However, the initial rate of recovery was approximately threefold higher in the parental samples than in the mutant samples (Fig. 4).

The decreased recovery of AO (green) fluorescence observed in CHL60-64 in vivo suggested that amine-induced vacuolation might be reduced in this cell line. This hypothesis was tested by microscopic examination of amine-treated cells. Vacuolation was monitored over time by phase contrast microscopy. Small vacuoles were observed within 20 min after addition of the amines in both cell types. With longer incubations, the parental cells developed large cytoplasmic vacuoles. The effect of 30 mM ammonia after 3 h is shown is Fig. 5 *b*. In contrast, much less vacuolation was seen in CHL60-64 (Fig. 5 *d*). Similar results were obtained with 100 mM ammonia and 60 μM chloroquine (data not shown).

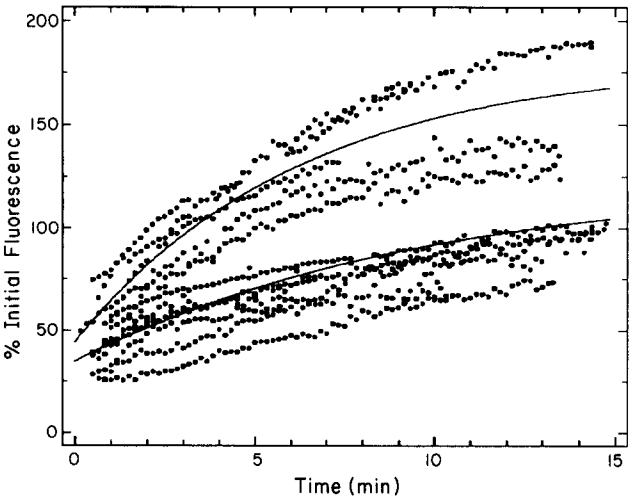

Figure 4. Effect of ammonium chloride on AO accumulation in vivo. The recovery of AO fluorescence (green) after the addition of NH_4Cl was measured for parental cells (*upper trace*) and CHL60-64 (*lower trace*). Cells were suspended in PBS/Ca/Mg by trypsinization, and AO was added to a concentration of 200 ng/ml (0.663 μM). The sample was incubated at 37°C until the AO fluorescence had stabilized (15 min). NH_4Cl was then added to a concentration of 100 mM, and fluorescence (488 nm excitation, 530 nm emission) monitored for 15 min. Green fluorescence decreased dramatically after NH_4Cl addition, then began to recover within 2 min. The data for multiple (five to seven) separate experiments are shown with fluorescence values normalized to percent of initial fluorescence. The data have also been aligned so that the start of the recovery period is plotted at 0 min. Each point represents the average of all events over a 10-s interval (~1,500 cells) for a single experiment. The line is an exponential function drawn using the average values for extent of recovery, extent of loss, and the average rate constant (it is not a least squares fit for the combined data for each cell type).

Although vacuolation was more extensive in both cell types with these higher concentrations of amines, vacuolation was always observed to be less in CHL60-64 than in the parental cells.

Ouabain Resistance

One possible mechanism for the observed reduction in acidification in CHL60-64 is through overexpression or missorting of pH-regulatory factors. The sodium- and potassium-activated adenosinetriphosphatase (Na^+/K^+-ATPase) has been postulated to be such a regulator (5). The presence of this ATPase in the very early, transferrin-containing endocytic compartments may limit the extent of acidification in these vesicles due to induction of an interior-positive membrane potential. Transport of these ATPases back to the plasma membrane along with recycling receptors would then allow acidification to proceed below pH 6 in late endosomes and lysosomes. If the sorting of the Na^+/K^+-ATPase were altered in CHL60-64 such that some ATPases were transported to lysosomes (as might result from overexpression of the ATPase), one might expect a decrease in the extent of acidification in the late, but not in the early, endocytic compartments. One prediction of this model is that CHL60-64 would have elevated levels of Na^+/K^+-ATPase. As an initial test of this possibility, the effect of ouabain (a potent inhibitor

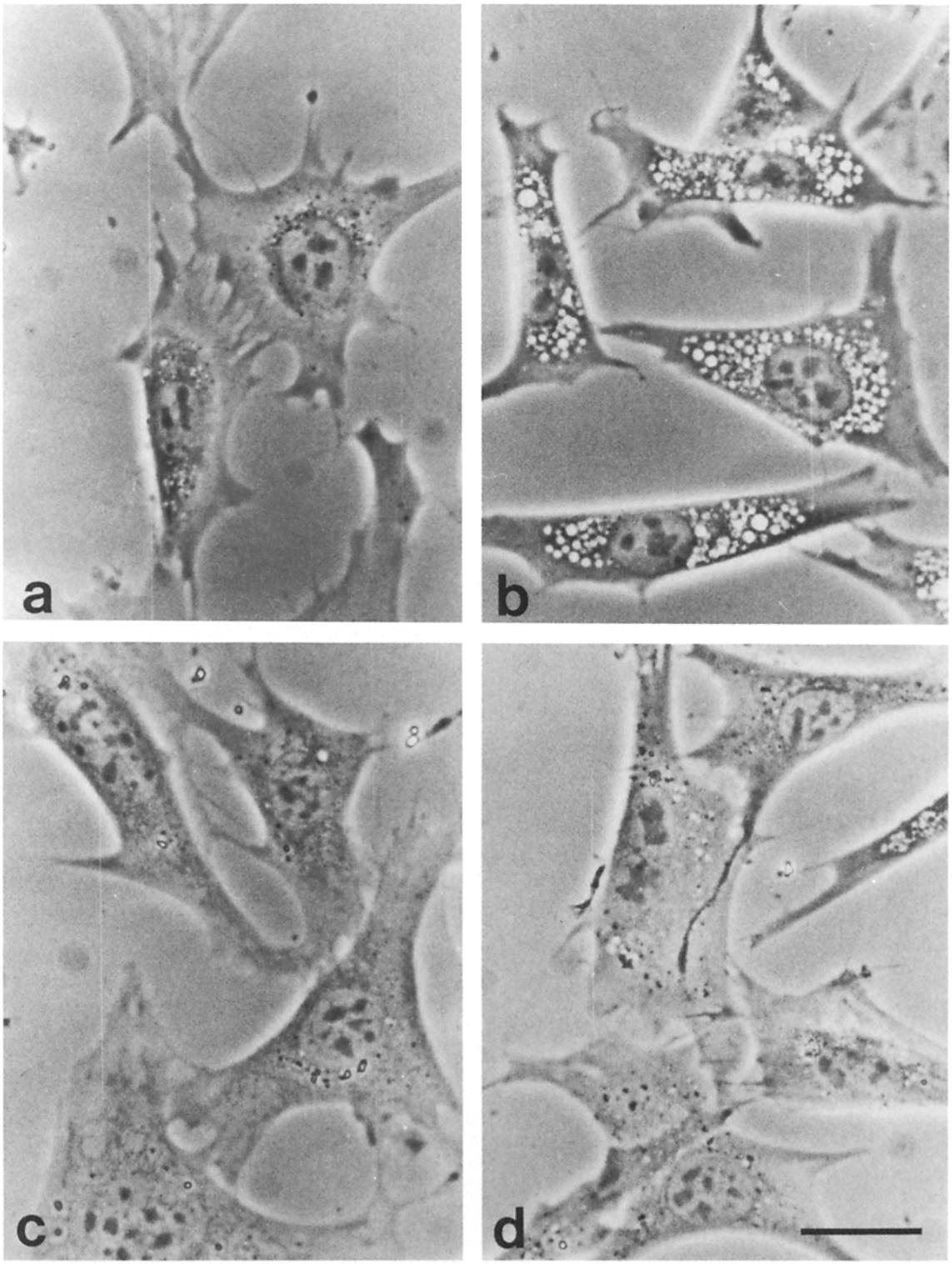

Figure 5. Amine induced vacuolation in parental and mutant cell lines. Parental cells (*a* and *b*) or CHL60-64 (*c* and *d*) were grown on slides and incubated in cDMEM with (*c* and *d*) or without (*a* and *b*) 30 mM ammonia for 3 h. Note the pronounced vacuolation in the parental cells in the presence of ammonia (*b*). Bar, 10 μm.

of the Na^+/K^+-ATPase) on the growth of CHL60-64 was examined (Fig. 6). This cell line is resistant to ouabain, relative to the parental cell line, as no cell death was seen at concentrations as high as 6 mM. In comparison, there were no surviving cells in the parental cultures at 3 mM ouabain. The correlation between acidification defects and ouabain resistance provides support for the postulated role of the Na^+/K^+-ATPase in endosomal pH regulation. Further support is

found in the observations that treatment with 1 mM ouabain eliminated the resistance of CHL60-64 to 60 μM chloroquine, and that short-term coincubation with both ouabain and chloroquine resulted in normal vacuolation (Cain, C. C., and R. F. Murphy, manuscript in preparation).

Discussion

Previous results have shown that an increase in intravesicular pH, caused by weak bases such as chloroquine, inhibits growth of cell cultures (2). This observation was used to isolate cell lines that were resistant to an increase in intravesicular pH. The isolated cell lines were resistant to chloroquine concentrations up to 60 μM, a concentration that increases the intravesicular pH to 6.0. Cell lines resistant to higher concentrations of chloroquine have been isolated, but were unstable with sudden cell death sometimes occurring after weeks of culture in 100 μM chloroquine. It is interesting that pH 6.0 is the apparent threshold for growth inhibition by chloroquine, tributylamine, benzylamine, and ammonium chloride (concentrations of the amines that increase the pH above 6.0 are toxic) (2).

Acidification of insulin (11), H-2K (12), epidermal growth factor (18), and dextran (17) has been shown to be biphasic, with an initial rapid acidification to approximately pH 6 (within 5 min), and a subsequent slow acidification to below pH 5.5. Transferrin follows the same initial kinetics of acidification but is recycled before the second phase of acidification (21). CHL60-64 exhibits normal early endocytic acidification, as shown by rapid acidification of transferrin after endocytosis to an extent equal to that in normal cells. However, subsequent acidification is slowed in this cell line. After 1 h, the average pH of endocytosed dextran in CHL60-64 is >6, while the dextrans are fully acidified in the parental cells by this time. The pH remains >5.8 for at least 4 h. However, late acidification is slowed, and not blocked, as the pH decreases to <5.5 by 8 h. This phenotype is different than those observed in other endocytic acidification mutants, which have been shown to have a defect in early acidification but not in lysosomal acidification.

Measurements of AO accumulation in whole cells and in isolated fractions indicate that there is a defect in CHL60-64 that decreases the extent to which some vesicles can be acidified. Although the extents of initial accumulation of AO by CHL60-64 and parental cell lines are very similar, the rates of uptake of AO after perturbation by 100 mM NH_4Cl are quite different. This is consistent with the defect seen in dextran acidification. The initial accumulation is due to the steady state proton gradient within the cell, and does not measure the rate of generation of these gradients. AO accumulation after perturbation, on the other hand, is an indirect measure of the rate of proton accumulation within cellular vesicles. The initial rate of recovery of green fluorescence after perturbation with 100 mM NH_4Cl in wild-type samples was three times the rate seen in the CHL60-64 samples. Vesicles isolated from CHL60-64 cells also exhibited an acidification defect in vitro. The initial rate of AO accumulation was 3.4-fold higher in lysosomal fractions, and 2.3-fold higher in endosomal fractions isolated from parental cells compared with fractions isolated from CHL60-64. Although this type of analysis does not measure the acidification of endocytic compartments per se, the acidification defect detected

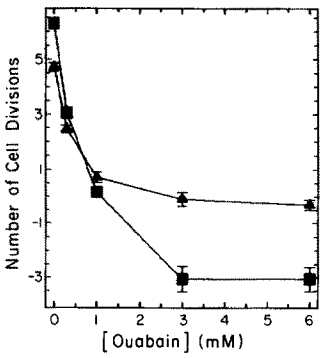

Figure 6. Ouabain resistance of CHL60-64. Actively growing cultures of high passage Swiss 3T3 (■) or CHL60-64 (▲) were incubated in the presence of various concentrations of ouabain for 4 d, and the number of cell divisions calculated relative to the number of cells at the time of ouabain addition. Each point represents the average and standard deviation of two counts each on duplicate plates; the data are representative of those from two separate experiments. Both cell types showed >90% viability (as judged by trypan blue exclusion) after treatment with 1 mM ouabain. While the vast majority of parental cells were killed by incubation with 3 mM ouabain, ~1 × 10^4 CHL60-64 cells remained after this treatment (>90% of these were viable).

supports the idea that the retarded lysosomal acidification observed using fluorescent dextrans is due to a defect in the acidification mechanism, not in transport.

The fact that endosomal fractions isolated from CHL60-64 show altered acidification kinetics is not inconsistent with the transferrin acidification data. Transferrin is rapidly internalized with other endocytic ligands, with acidification occurring very rapidly after internalization. After a brief exposure to mildly acidic pH (pH 6 in 3T3 cells [21]), the transferrin is sorted with its receptor into recycling vesicles, presumably with a number of other recycling molecules, and delivered to the cell surface. The material remaining in the endosome is further acidified at a slower rate, and is gradually found in dense lysosomes. It has previously been shown that the endosomal peak from a 27% (vol/vol) Percoll gradient (such as we have used here) can be resolved into two endosomal populations, one at a modal density of 1.035 and one at a density of 1.043, with the majority of the acid phosphatase activity of the endosome fraction found at 1.045 (10). Examination of the localization of epidermal growth factor in these endosomal fractions showed epidermal growth factor shifting from the lightest peak (1 min) into the heaviest peak (5 min) with time. In fractionation studies using ^{125}I-transferrin (23), internal transferrin migrated to a density of 1.03 while surface bound transferrin was found at a density of 1.02. Therefore, the acidification defect in CHL60-64 is presumably a defect in the acidification of the late compartments (heavy endosomes and lysosomes), but not the earliest, less dense endocytic compartments.

de Duve et al. (4) demonstrated that in order for amines to concentrate within cells to the extent measured for chloroquine, the loss of the proton gradient in lysosomes must be countered by active acidification. This is supported by our observations that the recovery of green AO fluorescence after addition of ammonium chloride is inhibited by metabolic poisons, and is temperature dependent. One consequence of active acidification in the presence of certain amines (chloroquine, methylamine, and ammonium chloride) is an increase in the osmotic pressure inside acidic vesicles due to trapping of the protonated forms of these weak bases. This leads to swelling of the vesicles, or vacuolation. Our data suggest

that the recovery of green fluorescence after amine perturbation is a measure of this swelling, and not regeneration of the proton gradient. First, the lysosomal pH as measured by FITC/XRITC-dextran does not recover within the same time period under the same conditions (data not shown). Second, no recovery of red fluorescence is seen, while the green fluorescence recovers to a level approximately twice the initial level. This indicates that the total cell-associated AO increases after addition of NH_4Cl, but that the concentration within each vesicle remains low.

When cells are selected for resistance to ouabain, one of the resulting phenotypes is an increase in the number of Na^+/K^+-ATPases in the plasma membrane (1). The ouabain resistance of CHL60-64 suggests that its acidification defect may be caused by a similar increase in number of Na^+/K^+-ATPases. It has been suggested by Fuchs et al. (5) that the acidification of the early endosome is limited by the presence of Na^+/K^+-ATPases that create a limiting membrane potential. It was further observed that the Na^+/K^+-ATPase does not seem to play a role in the acidification of late endosomes and lysosomes. If the recycling of these ATPases were partially defective in CHL60-64 (as might be caused by an increase in the number of molecules per cell), Na^+/K^+-ATPases would be present in late endocytic compartments and the extent of acidification in those compartments would be reduced. As these ATPases are removed (through sorting or degradation), the pH would gradually decrease to the lysosomal value.

To explain the amine resistance and acidification properties of CHL60-64, we postulate that proton pumping by the endosomal/lysosomal proton pump can be limited by either membrane potential or absolute pH. In both parental and mutant endosomes, the pH is regulated by membrane potential to pH 6. This is also the case for the majority of mutant lysosomes (as discussed above). In parental lysosomes, however, the membrane potential limitation is removed (due to absence of Na^+/K^+-ATPases), and proton pumping is postulated to be limited by absolute pH (to pH 5–5.5). In the presence of amine, parental lysosomes attempt to reestablish the original pH gradient, leading to increasing amine concentration and vacuolation. The mutant lysosomes, on the other hand, remain limited by membrane potential and do not vacuolate. Of course, those lysosomes in the mutant that have degraded (or otherwise removed) the Na^+/K^+-ATPases will behave like normal lysosomes and vacuolate; this explains the fact that the amine resistance (and resistance to vacuolation) of the mutant is not complete. In addition to protecting the mutant from vacuolation itself, the elimination of a futile cycle of attempted acidification may prevent the imposition of a large metabolic load on the cells.

It should be pointed out that molecules other than the Na^+/K^+-ATPase may be involved in the limitation of endosomal pH. It is anticipated that further characterization of the new class of mutants represented by CHL60-64, in combination with analysis of other acidification mutants, should provide information on the mechanism of endocytic pH regulation and allow the determination of the pH requirements of specific lysosomal functions in vivo.

We thank Mario Roederer and David Sipe for helpful discussions and critical reading of the manuscript, Ted Stamps for assistance in the isolation of chloroquine-resistant mutants, and Greg LaRocca, Del McCaslin, Denise Roush, Michael Silver, and Elizabeth Wickert for technical assistance.

This work was supported by National Institutes of Health grant GM 32508 and National Science Foundation Presidential Young Investigator Award DCB-8351364, with matching funds from Becton Dickinson Monoclonal Center, Inc.

Received for publication 26 March 1987, and in revised form 8 September 1987.

References

1. Ash, J. F., R. M. Fineman, T. Kalka, M. Morgan, and B. Wire. 1984. Amplification of sodium- and potassium-activated adenosinetriphosphatase in HeLa cells by ouabain step selection. *J. Cell Biol.* 99:971–983.
2. Cain, C. C., and R. F. Murphy. 1986. Growth inhibition of 3T3 fibroblasts by lysosomotropic amines: correlation with effects on intravesicular pH but not vacuolation. *J. Cell. Physiol.* 129:65–70.
3. De Belder, A. N., and K. Granath. 1973. Preparation and properties of fluorescein-labelled dextrans. *Carbohydr. Res.* 30:375–378.
4. de Duve, C., T. de Barsy, B. Poole, A. Trouet, P. Tulkens, and F. Van Hoof. 1974. Commentary. Lysosomotropic drugs. *Biochem. Pharmacol.* 23:2495–2531.
5. Fuchs, R., S. Schmid, P. Male, A. Helenius, and I. Mellman. 1986. Isolation and ATP-dependent acidification of endosome subcompartments from CHO cells. *J. Cell Biol.* 103:439*a*. (Abstr.).
6. Klausner, R. D., J. van Renswoude, C. Kempf, K. Rao, J. L. Bateman, and A. R. Robbins. 1984. Failure to release iron from transferrin in a Chinese hamster ovary cell mutant pleiotropically defective in endocytosis. *J. Cell Biol.* 98:1098–1101.
7. Marnell, M. H., L. S. Mathis, M. Stookey, S.-P. Shia, D. K. Stone, and R. K. Draper. 1984. A Chinese hamster ovary cell mutant with a heat-sensitive, conditional-lethal defect in vacuolar function. *J. Cell Biol.* 99:1907–1916.
8. Marsh, M., E. Bolzau, and A. Helenius. 1983. Penetration of semliki forest virus from acidic prelysosomal vacuoles. *Cell.* 32:931–940.
9. Merion, M., P. Schlesinger, R. M. Brooks, J. M. Moehring, T. J. Moehring, and W. S. Sly. 1983. Defective acidification of endosomes in Chinese hamster ovary cell mutants "cross-resistant" to toxins and viruses. *Proc. Natl. Acad. Sci. USA.* 80:5315–5319.
10. Merion, M., and W. S. Sly. 1983. The role of intermediate vesicles in the adsorptive endocytosis and transport of ligand to lysosomes by human fibroblasts. *J. Cell Biol.* 96:644–650.
11. Murphy, R. F., S. Powers, and C. R. Cantor. 1984. Endosomal pH measured in single cells by dual fluorescence flow cytometry: rapid acidification of insulin to pH 6. *J. Cell Biol.* 98:1757–1762.
12. Murphy, R. F., D. B. Tse, C. R. Cantor, and B. Pernis. 1984. Acidification of internalized class I major histocompatibility complex antigen by T lymphblasts. *Cell. Immunol.* 88:336–342.
13. Ono, M., K. Mifune, A. Yoshimura, S. Ohnishi, and M. Kuwano. 1985. Monensin-resistant mouse BALB/3T3 cell mutant with aberrant penetration of vesicular stomatitis virus. *J. Cell Biol.* 101:60–65.
14. Poole, B., and S. Ohkuma. 1981. Effect of weak bases on the intralysosomal pH in mouse peritoneal macrophages. *J. Cell Biol.* 90:665–669.
15. Robbins, A. R., C. Oliver, J. L. Bateman, S. S. Krag, C. J. Galloway, and I. Mellman. 1984. A single mutation in Chinese hamster ovary cells impairs both Golgi and endosomal function. *J. Cell Biol.* 99:1296–1308.
16. Robbins, A. R., S. S. Peng, and J. L. Marshall. 1983. Mutant Chinese hamster ovary cells pleiotropically defective in receptor-mediated endocytosis. *J. Cell Biol.* 96:1064–1071.
17. Roederer, M., B. Bowser, and R. F. Murphy. 1987. Kinetics and temperature dependence of exposure of endocytosed material to proteolytic enzymes and low pH: evidence for a maturation model for the formation of lysosomes. *J. Cell. Physiol.* 131:200–209.
18. Roederer, M., and R. F. Murphy. 1986. Cell-by-cell autofluorescence correction for low signal-to-noise systems: application to EGF endocytosis by 3T3 fibroblasts. *Cytometry.* 7:558–565.
19. Roff, C. F., R. Fuchs, I. Mellman, and A. R. Robbins. 1986. Chinese hamster ovary cell mutants with temperature-sensitive defects in endocytosis. I. Loss of function on shifting to the nonpermissive temperature. *J. Cell Biol.* 103:2283–2297.
20. Sandvig, K., and S. Olsnes. 1980. Diphtheria toxin entry into cells is facilitated by low pH. *J. Cell Biol.* 87:828–832.
21. Sipe, D. M., and R. F. Murphy. 1987. High resolution kinetics of transferrin acidification in BALB/c 3T3 cells: exposure to pH 6 followed by temperature-sensitive alkalinization during recycling. *Proc. Natl. Acad. Sci. USA.* 84:7119–7123.
22. Timchak, L. M., F. Kruse, M. H. Marnell, and R. K. Draper. 1986. A thermosensitive lesion in a Chinese hamster cell mutant causing differential effects on the acidification of endosomes and lysosomes. *J. Biol.*

Chem. 261:14154–14159.

23. van Renswoude, J., K. R. Bridges, J. B. Harford, and R. D. Klausner. 1982. Receptor-mediated endocytosis of transferrin and the uptake of Fe in K652 cells: identification of a nonlysosomal acidic compartment. *Proc. Natl. Acad. Sci. USA.* 79:6186–6190.
24. Yoshimura, A., K. Kuroda, K. Kawasaki, S. Yamashima, T. Maeda, and S. Ohnishi. 1982. Infectious cell entry mechanism of influenza virus. *J. Virol.* 43:284–293.